

In vivo evaluation of the dopaminergic neurotransmission system using [¹²³I]FP-CIT SPECT in 6-OHDA lesioned rats

Aida Niñerola-Baizán^{a,b}, Santiago Rojas^c, Mercè Bonastre^d, Raúl Tudela^b, Francisco Lomeña^{e,f,g}, Javier Pavía^{b,e,g}, Concepció Marin^{d,h} and Domènec Ros^{a,b,g,*}

The 6-hydroxydopamine (6-OHDA) rodent model of Parkinson's disease (PD) has been used to evaluate the nigrostriatal pathway. The aim of this work was to explore the relationship between the degree of 6-OHDA-induced dopaminergic degeneration and [¹²³I]FP-CIT binding using single photon emission computed tomography (SPECT). Fourteen rats received a 6-OHDA injection (4 or 8 µg) into the left medial forebrain bundle. After 3 weeks, magnetic resonance imaging and scans with a small-animal SPECT system were performed. Finally, the nigrostriatal lesion was assessed by immunohistochemical analysis. Immunohistochemical analysis confirmed two levels of dopaminergic degeneration. Lesions induced by 6-OHDA diminished the ipsilateral [¹²³I]FP-CIT binding by 61 and 76%, respectively. The decrease in tracer uptake between control and lesioned animals was statistically significant, as was the difference between the two 6-OHDA lesioned groups. Results concluded that [¹²³I]FP-CIT SPECT is a useful technique to discriminate the degree of dopaminergic degeneration in a rat model of PD. Copyright © 2014 John Wiley & Sons, Ltd.

Keywords: [¹²³I]FP-CIT; 6-OHDA; SPECT; rat; Parkinson's disease; molecular imaging

1. INTRODUCTION

Single photon emission computed tomography (SPECT) has become a useful neuroimaging technique for *in vivo* evaluation of neurotransmission systems in both clinical diagnosis (1) and basic research (2). Specifically, SPECT allows the evaluation of presynaptic dopaminergic terminals of the nigrostriatal neurotransmission system.

Presynaptic dopamine function is associated with the dopamine transporter (DAT). The DAT is responsible for reuptake of dopamine from the synaptic cleft and has proved to be a sensitive indicator of the nigrostriatal dopaminergic function. Parkinson's Disease (PD) is related to a degeneration of the nigrostriatal dopaminergic system and SPECT with [¹²³I]-N-omega-fluoropropyl-2β-carbomethoxy-3β-(4-iodophenyl)nortropine ([¹²³I]FP-CIT, DaTSCAN; GE Healthcare), a radiotracer that binds DAT, has been shown to be useful for PD diagnosis (1,3).

The fact that the same tracer can be employed in animal models and in humans allows translational research. By studying models of PD using [¹²³I]FP-CIT SPECT, an increasing number of compounds with neuroprotective properties (4) could be examined along with other therapeutic approaches (5) in PD treatment.

A good correlation between [¹²³I]FP-CIT SPECT and histopathology in relation to dopaminergic degeneration has been found using the neurotoxin 1-methyl-4-phenyl-1,2,3,6-tetrahydropyridine in monkeys (6) and mice (7). PD rodent models using the neurotoxin 6-hydroxydopamine (6-OHDA) have also been reported (8–12). This model of PD has been widely used in studies exploring the effect of different treatments by histochemical evaluation of nigral tyrosine hydroxylase (TH) and/or striatal DAT

(13–17). Molecular imaging techniques have also been applied to this model of dopaminergic degeneration. Although several studies have used positron emission tomography to evaluate

* Correspondence to: D. Ros, Unitat de Biofísica i Bioenginyeria, Facultat de Medicina, Universitat de Barcelona, Barcelona, Spain. E-mail: dros@ub.edu

a A. Niñerola-Baizán, D. Ros
Unitat de Biofísica i Bioenginyeria, Facultat de Medicina, Universitat de Barcelona, Barcelona, Spain

b A. Niñerola-Baizán, R. Tudela, J. Pavía, D. Ros
Centro de Investigación Biomédica en Red de Bioingeniería, Biomateriales y Nanomedicina, Barcelona, Spain

c S. Rojas
Thrombotargets Europe S.L., Castelldefels, Spain

d M. Bonastre, C. Marin
INGENIO, IRCE, Institut d'Investigacions Biomèdiques August Pi i Sunyer, Barcelona, Spain

e F. Lomeña, J. Pavía
Servei de Medicina Nuclear, Hospital Clínic, Barcelona, Spain

f F. Lomeña
Centro de Investigación Biomédica en Red de Salud Mental, Barcelona, Spain

g F. Lomeña, J. Pavía, D. Ros
Institut d'Investigacions Biomèdiques August Pi i Sunyer, Barcelona, Spain

h C. Marin
Centro de Investigación Biomédica en Red de Enfermedades Neurodegenerativas, Barcelona, Spain

6-OHDA-induced lesions in rats (18–25), very few studies examining DAT binding have been carried out with this animal model using SPECT (26–31).

Along these lines, a very recently published work has confirmed a correlation between histopathological lesion and DAT SPECT measurements using the radiotracer [^{123}I] β -CIT in rats subjected to different intrastriatal administrations of 6-OHDA (29). In parallel to this study, we have evaluated a 6-OHDA rat model using immunohistochemistry, magnetic resonance imaging (MRI) and [^{123}I] β -CIT SPECT. Whereas previous studies performed in similar rat models of PD used [^{123}I] β -CIT, we chose the radiotracer [^{123}I] β -CIT, as it presents a faster kinetics and is currently the radiotracer of choice in human studies for the evaluation of PD and other neurological disorders of basal ganglia (2,3,32). Thus, while preclinical SPECT studies can also be performed using other radiotracers binding DAT, the extensive clinical use of [^{123}I] β -CIT makes it a very interesting tool for translational research in this area. The ability to explore, detect and discriminate different degrees of nigrostriatal degeneration in rats subjected to 6-OHDA injection in the medial forebrain bundle (MFB) is a positive asset.

The aim of this work was to confirm the relationship between the degree of dopaminergic degeneration (evidenced by the behavior and histology) and neuroimaging [^{123}I] β -CIT SPECT on an experimental rat model of PD. To this end, two levels of dopaminergic degeneration were induced by administering 6-OHDA at increasing doses into the left MFB (10,33). This approach induces a reproducible unilateral degeneration of dopaminergic terminals in the striatum without the mechanical injury that inevitably occurs when 6-OHDA is injected directly into the basal ganglia.

2. MATERIALS AND METHODS

2.1. 6-OHDA Lesions

Male Sprague–Dawley rats weighing 220–240 g were housed on a 12 h light/dark cycle with free access to food and water. Under sodium pentobarbital anesthesia (50 mg/kg, i.p.), the animals were placed in a stereotaxic frame with the incisor bar positioned 4.5 mm below the interaural line. Two degrees of unilateral nigrostriatal degeneration (total or partial) were induced. Each animal received a 6-OHDA injection (8 or 4 μg in 4 μl of saline with 0.02% ascorbate over 8 min for total $n=7$ or partial lesion $n=4$, respectively) (34–36) into the MFB by means of a Harvard infusion pump. Control animals received the same volume of vehicle in the left MFB ($n=4$). Stereotaxic injections were placed 4.0 mm anterior to the interaural line, 1.3 mm lateral to the midline and 8.4 mm ventral to the surface of the skull, according to the atlas of Paxinos and Watson (37). All animal experiments were carried out in accordance with the National Institute of Health guide for care and use of laboratory animals and were approved by local governmental authorities.

2.2. Rotational Screening

For the measurement of rotational behavior, animals were placed in circular cages and tethered to an automated rotometer. The number of complete (360°) turns made during each 5-minute period was automatically recorded by a computerized system. Animals were allowed to become habituated to the rotometer for 15 min before apomorphine (0.05 mg/kg, subcutaneous, s.c.) administration. Following a 3 week recovery

period, animals exhibiting rotational response (>100 total turns for a total and <70 total turns for a partially lesioned animal) over a 45 min test session were selected for further study (38).

2.3. Magnetic Resonance Imaging

Three weeks after the induction of the lesion, T_1 -weighted MRIs were obtained for all animals to provide anatomic landmarks for region of interest (ROI) definition and for its positioning on SPECT images (35). Additionally, T_2 -weighted images and apparent diffusion coefficient (ADC) maps were obtained in order to evaluate the occurrence of edema, hemorrhage or other major alterations in the striatum and injection area.

MRI experiments were conducted using a 7.0 T BioSpec 70/30 horizontal animal scanner (Bruker BioSpin, Ettlingen, Germany), equipped with a 12 cm inner diameter actively shielded gradient system (400 mT/m). The receiver coil was a phased array surface coil for the animal brain. Animals were placed in supine position in a Plexiglas holder with a nose cone for anesthesia administration (2% isoflurane in a mixture of oxygen and N_2O at a 30:70 ratio) and fixed by a tooth bar, ear bars and adhesive tape. Tripilot scans were carried out for accurate positioning of the animal's head in the isocenter of the magnet.

2.4. Apparent Diffusion Coefficient Maps

ADC scans were acquired using a pulsed gradient spin echo sequence with the following acquisition parameters: echo time (TE) = 55.07 ms, repetition time (TR) = 50000 ms, with a total acquisition time of 2 min 20 s, six b -values from 100 to 1000 s/mm^2 , a field of view (FOV) = $40 \times 40 \times 30 \text{ mm}^3$, with a matrix size of $128 \times 128 \times 20$ pixels and a spatial resolution of $0.312 \times 0.312 \times 1.5 \text{ mm}/\text{pixel}$.

2.5. T_2 Maps

T_2 scans were acquired with a multi-slice multi-echo sequence by applying 16 different TE s, from 11 to 176 ms, $TR = 4764$ ms, slice thickness = 1.5 mm, number of slices = 20, $FOV = 40 \times 40 \text{ mm}$ and matrix size = 256×256 pixels, resulting in a spatial resolution of $0.156 \times 0.156 \text{ mm}$ in 1.5 mm slice thickness.

2.6. T_1 Weighted

High-resolution anatomical scans were obtained with a T_1 -weighted high resolution 3D MRI with a modified driven equilibrium Fourier transform sequence with $TE = 3.5$ ms, with eight segments, TR segment = 4000 ms, two averages, a total acquisition time of 1 h 4 min, slice thickness 0.5 mm, number of slices 60, $FOV = 40 \times 40 \text{ mm}$, and matrix size 256×256 pixels, resulting in a spatial resolution of $0.156 \times 0.156 \times 0.5 \text{ mm}/\text{pixel}$.

2.7. SPECT Imaging

Three weeks after the induction of the lesion, all scans were performed with a dedicated small-animal SPECT system (39) (2 mm intrinsic resolution) equipped with a low-energy high-resolution parallel-hole collimator. SPECT scanning started 30 min after intravenous injection of $90 \pm 5 \text{ MBq}$ of [^{123}I] β -CIT into the tail vein, which is the pseudoequilibrium time, in accordance with previous published data (40). For dose injection and SPECT acquisition, animals were maintained under anesthesia with isoflurane at 1.5% in oxygen. Data were acquired for 60 min in a step-and-shoot mode over a circular

orbit in angular steps of 6° (60 projections, 60 s/projection) and a rotation radius of 30 mm. A 15% energy window was centered on the 159 keV energy photons, the main emission line of ¹²³I (97% yield).

2.8. Tissue Collection

Animals were sacrificed by overdose of pentobarbital anesthesia 5 days after SPECT scan. Brains were quickly removed from the skull and then frozen on dry ice and kept at -80°C until they were cut on a cryostat. Coronal 14 µm thick sections from the striatal region were obtained with a cryomicrotome and collected onto APTS (3-amino-propyltriethoxysilane) coated slides. The obtained sections were kept at -40°C until used.

2.9. DAT and TH Immunohistochemistry

Sections were thawed, dried at room temperature and fixed with acetone for 10 min at 4°C. After that, they were rinsed twice in phosphate-buffered saline (PBS; 1×, pH 7.4) for 5 min, and immersed in a PBS solution of 0.3% hydrogen peroxide for 10 min to block the endogenous peroxidases. Sections were then rinsed in PBS 1× and incubated for 20 min in a blocking solution containing horse serum (1:10) and 0.1% Triton X-100. Sections were incubated overnight at 4°C with mouse anti-DAT or anti-TH antibodies (Santa Cruz Biotechnology Inc, CA, USA) at dilutions of 1:500 and 1:5000 in PBS, respectively. Finally, the immunohistochemistry was developed using ImmunoPure Ultra-Sensitive ABC Peroxidase staining kit (Vector, UK), dehydrated and mounted in Distrene Plasticiser Xylene (DPX) for microscopic evaluation.

2.10. SPECT Image Quantification

Projections were filtered with a 2D-Butterworth filter (3.13/cm, order 5). Then, reconstruction was performed using filtered back projection algorithm with a ramp filter. A 128 × 128 × 100 matrix size and 0.32 × 0.32 × 0.32 mm³ voxel size were used (41).

MRI was automatically realigned using Statistical Parametric Mapping (SPM, The Wellcome Department of Imaging Neuroscience, London, UK; www.fil.ion.ucl.ac.uk/spm) to the reference MRI, which was coregistered to the Rubins rat brain atlas (42). Afterwards, each SPECT image was manually coregistered to its MRI to confirm the anatomical location of the striatal uptake.

ROIs were drawn on the reference MRI with the backing of anatomical information from both the Rubins rat brain atlas

and the MR image and applied to the coregistered SPECT image. A reference ROI was defined on the global brain excluding the striatum in order to obtain nonspecific uptake. We decided on this reference ROI rather than using the cerebellum, which has been used in a number of studies, because of the low specific binding of [¹²³I]FP-CIT in sites other than DAT in striatum. The use of such an extended region of no specific uptake helped diminish variability owing to noise in specific uptake ratio (SUR) calculation and yielded highly comparable results. This is important in experiments with a reduced number of animals, as reported in the present work.

Striatal binding was evaluated by the SUR, which was calculated as $SUR = (S - B)/B$, where S is the concentration activity (counts/ml) in the striatum and B that of the background reference region.

2.11. Statistical Analysis

Obtained SUR values and their ratios were analyzed using one-way ANOVA and Bonferroni *post-hoc* test. Results from partial and total lesions were also analyzed using a Student's *t*-test. In all cases $p < 0.05$ was considered statistically significant.

3. RESULTS

3.1. Rotational Screening

Animals that received 6-OHDA were classified into two groups according to the results of rotational screening. Those exhibiting fewer than 70 contralateral rotations were classified as partially lesioned animals ($n = 4$) and those showing more than 100 contralateral rotations formed the totally lesioned group ($n = 7$).

3.2. Magnetic Resonance Imaging

Images obtained from all the animals were equivalent and no differences were observed between MR images from the three groups under study. No changes in image intensity were observed at the level of ipsilateral striatum or MFB in any acquired sequence. In all cases, the lesion produced by the needle used for injection can be seen in the T_1 -weighted image. No other structural alterations suggestive of secondary hemorrhage, infection, cytotoxic or vascular edema were found (Fig. 1).

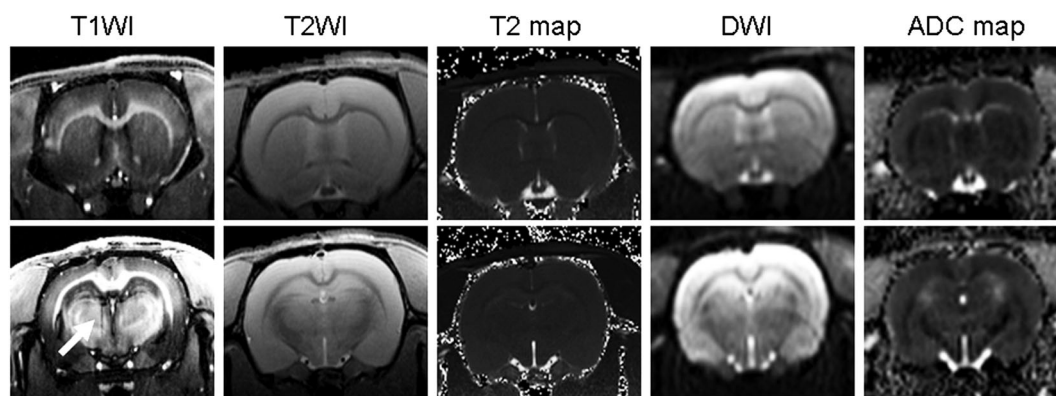


Figure 1. Representative MR images obtained from a rat subjected to total lesion. T_1 - and T_2 -weighted images, T_2 map, diffusion-weighted image and apparent diffusion coefficient (ADC) map are shown. Images in the upper and lower rows were obtained at striatum level and at the level of injection area, respectively. The white arrow indicates the lesion produced during 6-OHDA administration.

3.3. DAT and TH Immunohistochemistry: Characterization of the Unilateral 6-OHDA Lesion

As expected for a total 6-OHDA lesion of the nigrostriatal pathway, nigral TH and striatal DAT-immunoreactivities in the ipsilateral hemisphere were absent in this group of animals. A partial loss of nigral TH and striatal DAT immunoreactivities was observed in the partially lesioned animals (Fig. 2).

3.4. SPECT Image Quantification: Uptake of [¹²³I]FP-CIT

On visual inspection, high [¹²³I]FP-CIT uptake was observed at the regions corresponding to Harder's glands, thyroid gland

and striatum. Figure 3 shows representative SPECT images overlaid with the MRI for a control, a partially lesioned and a totally lesioned animal. A symmetrical striatal [¹²³I]FP-CIT distribution was observed in the control. In contrast, in both lesioned animals, [¹²³I]FP-CIT uptake was lower in the ipsilateral striatum. This asymmetry was more pronounced in the totally lesioned animal.

Image quantification showed contralateral average SUR values of 0.60 ± 0.14 , 0.66 ± 0.09 and 0.69 ± 0.27 for control, partially lesioned and totally lesioned animals, respectively. In contrast, corresponding ipsilateral SUR values decreased to 0.23 ± 0.06 in partially lesioned and to 0.14 ± 0.08 in totally lesioned rats (Fig. 4a). In the same way, mean values of the ipsilateral to

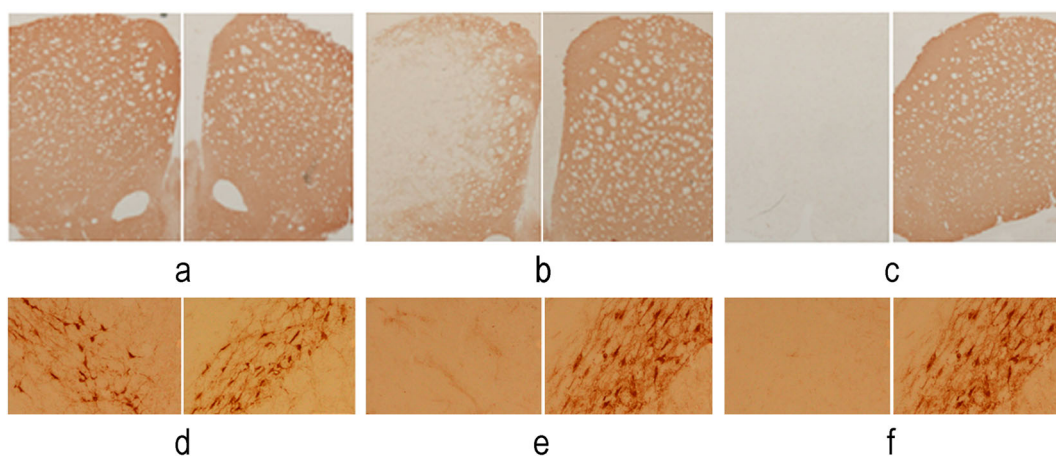


Figure 2. Images of striatal dopamine transporter (DAT; top) and nigral tyrosine hydroxylase (TH; bottom) immunohistochemistry from 14 μm coronal section for control (a, d), partially lesioned (b, e) and totally lesioned (c, f) animals. Each pair of images represents contra- (right) and ipsilateral (left) hemispheres. Magnification (in d–f) = 20 \times .

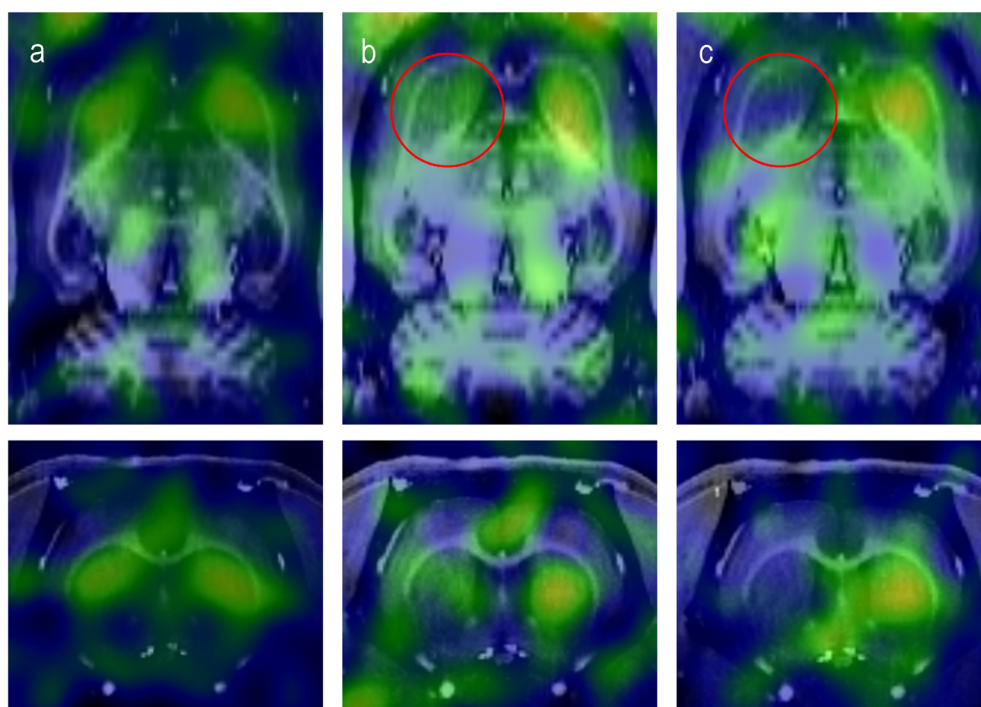


Figure 3. Axial (top) and coronal (below) views of [¹²³I]FP-CIT SPECT image overlaid with MRI showing [¹²³I]FP-CIT uptake in a control (a), partially lesioned (b) and totally lesioned rat (c).

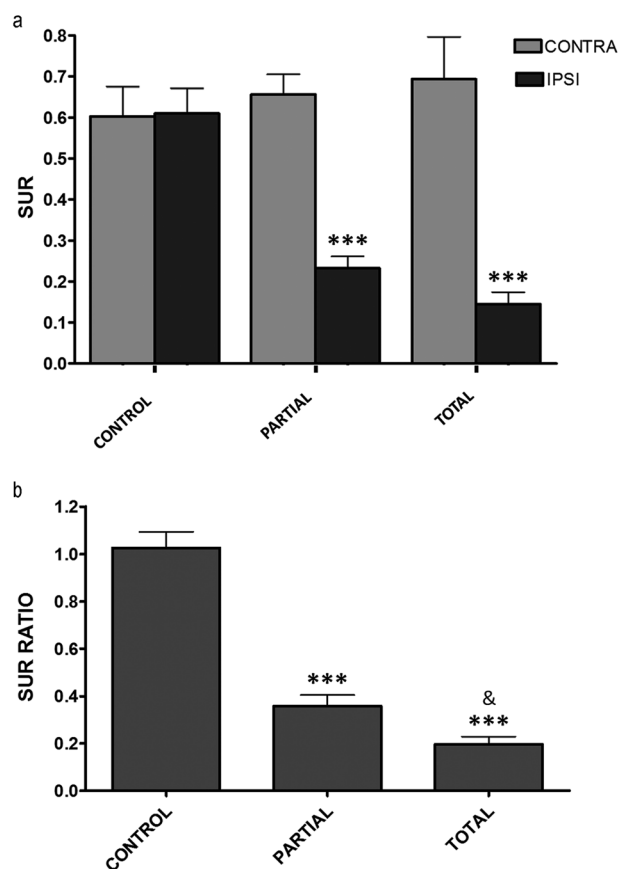


Figure 4. Results from image quantification showing the decrease in the ipsilateral striatum in partially and totally lesioned animals. (a) specific uptake ratio (SUR) values obtained for ipsilateral and contralateral striatum in the three groups. One-way ANOVA, $p < 0.001$. *** Bonferroni *post-hoc* test vs control, $p < 0.001$. (b) Ipsilateral contralateral SUR ratios. One-way ANOVA, $p < 0.001$. *** Bonferroni *post-hoc* test vs control, $p < 0.001$. & Student's *t*-test partial vs total, $p = 0.0173$.

contralateral SUR ratios for control, partially lesioned and totally lesioned animals were 1.03 ± 0.14 , 0.36 ± 0.09 and 0.20 ± 0.08 , respectively (Fig. 4b).

Statistical analysis showed that uptake of $[^{123}\text{I}]\text{FP-CIT}$ computed as SUR was equivalent in the contralateral striatum of the three groups. In contrast, SUR values in ipsilateral striatum were significantly reduced in both partially and totally lesioned animals (one-way ANOVA, $p < 0.001$; Bonferroni *post-hoc* test vs control, $p < 0.001$; Fig. 4a). The ipsilateral to contralateral SUR ratios were also significantly reduced in both groups of lesioned animals when compared to controls (one-way ANOVA, $p < 0.001$; Bonferroni *post-hoc* test vs control, $p < 0.001$). Moreover, the animals affected by total lesions presented a significantly lower SUR ratio than partially lesioned animals (Student's *t*-test partial vs total, $p = 0.0173$), and this was consistent with immunostaining results (Fig. 4b).

4. DISCUSSION

The 6-OHDA lesion model of PD is widely used in studies designed to assess the effect of different treatments by histochemical evaluation of nigrostriatal tract and/or neuroimaging techniques. In these studies, rats subjected to intrastratial

administration of 6-OHDA were evaluated with SPECT and the radiotracer $[^{123}\text{I}]\beta\text{-CIT}$. To our knowledge, however, until now the degree of dopaminergic degeneration in this animal model has not been evaluated using the radiotracer $[^{123}\text{I}]\text{FP-CIT}$. Its faster kinetics facilitate clinical studies and it is currently the most widely used SPECT radiotracer for PD diagnosis. Although results obtained with $[^{123}\text{I}]\text{FP-CIT}$ are likely to be similar to those of $[^{123}\text{I}]\beta\text{-CIT}$, validation of its ability to detect different degrees of dopaminergic degeneration is required before further use in pre-clinical PD research. Interestingly, one recently published work has analyzed the effect of long-term treatment with levodopa or the dopamine agonist pramipexole using $[^{123}\text{I}]\text{FP-CIT}$ SPECT combined with histochemistry on 6-OHDA lesioned mice (34). Although SPECT can be used to evaluate mice, resolution issues make a rat model more suitable than mouse for longitudinal *in vivo* evaluation by molecular imaging. In addition, their larger size can also be an advantage when testing a variety of therapeutic interventions, such as electrode placement, surgical intervention to the brain or intraventricular administration of compounds.

Immunohistochemistry results for DAT and TH in Fig. 2 confirm that two levels (partial and total) of dopaminergic degeneration occurred in rats. As expected, absence and a partial loss of nigral TH and striatal DAT-immunoreactivities in the ipsilateral hemisphere were noticed in the group of totally and partially lesioned animals, respectively. Moreover, injecting the 6-OHDA into the MFB instead of striatum could be advantageous to evaluate the relationship between induced dopaminergic degeneration and the radiotracer binding. In fact, in previous published works the neurotoxic drug was injected in the striatum (29). This inevitably causes a mechanical disturbance in the injected area that could produce secondary alterations that may in turn affect radiotracer uptake. Injecting the neurotoxic drug at the level of MFB causes a reproducible degeneration of nigrostriatal tract, avoiding other disturbances in the radiotracer binding area. In addition, MRI evaluation indicated that, at least at the time of evaluation, the animals did not present cytotoxic or vasogenic edema, hemorrhage or infection associated with 6-OHDA administration and the posterior degeneration of dopaminergic terminals in the striatum. These alterations occur in other pathologic situations like brain infarction and could influence radiotracer kinetics in the lesioned area (43). In this way, it can be speculated that cytotoxic or vasogenic edema could occur during the acute phase of 6-OHDA administration and this might affect the binding of radiotracer. However, a longitudinal evaluation of $[^{123}\text{I}]\text{FP-CIT}$ binding during the development of nigrostriatal degeneration is beyond the scope of this paper.

This study demonstrates that SPECT with $[^{123}\text{I}]\text{FP-CIT}$ can be used to discriminate different degrees of dopaminergic lesion. Thus, while a symmetrical striatal $[^{123}\text{I}]\text{FP-CIT}$ distribution was seen in control animals, in partially lesioned animals its $[^{123}\text{I}]\text{FP-CIT}$ uptake was lower in the ipsilateral striatum. This asymmetry increased in totally lesioned animals. SUR values obtained by SPECT image quantification revealed that partial and total lesions led to a 61 and 76% decrease in $[^{123}\text{I}]\text{FP-CIT}$ binding, respectively. An interesting collateral point is the fact that the level of contralateral binding increases with the degree of lesion (Fig. 4a). Although this increment is not statistically significant, it could be caused by a compensatory mechanism of the contralateral striatum in response to the loss of nigrostriatal innervation of ipsilateral ganglia. Similar compensatory mechanisms have been described by other authors (44).

Our results are in agreement with those reported in a recent SPECT study where [¹²³I]β-CIT was used (29). In that study, 6-OHDA was administered to the rat striatum. As opposed to injection directly into the basal ganglia, MFB injections induce reproducible unilateral degeneration of dopaminergic terminals in the striatum while avoiding mechanical injury, making them more suitable for radiotracer evaluation. The study also reported that [¹²³I]β-CIT/CT showed a high correlation to immunohistochemical findings, confirming its use to estimate the severity of the 6-OHDA lesion. Moreover, since [¹²³I]FP-CIT is used more often in clinical evaluation of movement disorders than [¹²³I]β-CIT, its characterization in animal models is highly desirable. In fact, the evaluation of this radiotracer in the 6-OHDA rat model paves the way for further use of SPECT with [¹²³I]FP-CIT in preclinical development of therapeutic strategies for PD and other related pathologies.

In summary, our findings confirm the relationship between the degree of dopaminergic degeneration (evidenced by behavior and histology) and neuroimaging obtained with [¹²³I]FP-CIT SPECT, showing that the sensitivity of this approach allows different levels of nigrostriatal degeneration to be distinguished in a 6-OHDA PD experimental rat model.

5. CONCLUSIONS

SPECT with [¹²³I]FP-CIT enables the *in vivo* evaluation of different degrees of dopaminergic degeneration in rats that have been lesioned by 6-OHDA administration to the MFB.

Acknowledgments

This work was supported in part by the Spanish Ministry of Science and Innovation (SAF2009-08076), CDTI-CENIT (AMIT project), Fondo de Investigaciones Sanitarias (PI12-00390) and CIBER-BBN, as an initiative funded by the VI National R&D&I Plan 2008–2011, Iniciativa Ingenio 2010, Consolider Program, CIBER Actions and financed by the Instituto de Salud Carlos III with assistance from the European Regional Development Fund. We are indebted to Guadalupe Soria and Xavier López-Gil from the Experimental MRI 7 T Unit of the Institut d'Investigacions Biomèdiques August Pi i Sunyer for their technical help.

REFERENCES

- Acton PD, Choi SR, Plossl K, Kung HF. Quantification of dopamine transporters in the mouse brain using ultrahigh resolution SPECT. *Eur J Nucl Med Mol Imag* 2002; 29: 691–698.
- Tatsch K. Imaging of the dopaminergic system in parkinsonism with SPET. *Nucl Med Commun* 2001; 22: 819–827.
- Booij J, Tissingh G, Winogrodzka A, van Royen EA. Imaging of the dopaminergic neurotransmission SPECT and positron emission tomography in patients with parkinsonism. *Eur J Nucl Med* 1999; 26: 171–182.
- Marin C, Aguilar E, Obeso JA. Coadministration of entacapone with levodopa attenuates the severity of dyskinesias in hemiparkinsonian rats. *Mov Disord* 2006; 21: 645–653.
- Kim JH, Auerbach JM, Rodríguez-Gómez JA, Velasco I, Gavin D, Lumelsky N, Lee SH, Nguyen J, Sánchez-Pernaute R, Bankiewicz K, McKay R. Dopamine neurons derived from embryonic stem cells function in an animal model of Parkinson's disease. *Nature* 2002; 418: 50–56.
- Ashkan K, Wallace BA, Mitrofanis J, Pollo C, Brard PY, Fagret D, Benabid AL. SPECT imaging, immunohistochemical and behavioural correlations in the primate models of Parkinson's disease. *Parkinsonism Relat Disord* 2007; 13: 266–275.

- Alvarez-Fischer D, Blessmann G, Trosowski C, Béhé M, Schurrat T, Hartmann A, Behr TM, Oertel WH, Höglinger GU, Höffken H. Quantitative [(123)I] FP-CIT pinhole SPECT imaging predicts striatal dopamine levels, but not number of nigral neurons in different mouse models of Parkinson's disease. *Neuroimage* 2007; 38: 5–12.
- Ungerstedt U. 6-Hydroxy-dopamine induced degeneration of central monoamine neurons. *Eur J Pharmacol* 1968; 5: 107–110.
- Schwartz RK, Huston JP. The unilateral 6-hydroxydopamine lesion model in behavioral brain research. Analysis of functional deficits, recovery and treatments. *Prog Neurobiol* 1996; 50: 275–331.
- Deumens R, Blokland A, Prickaerts J. Modeling Parkinson's disease in rats: an evaluation of 6-OHDA lesions of the nigrostriatal pathway. *Exp Neurol* 2002; 175: 303–317.
- Duty S, Jenner P. Animal models of Parkinson's disease: a source of novel treatments and clues to the cause of the disease. *Br J Pharmacol* 2011; 164: 1357–1391.
- Blandini F, Armentero MT. Animal models of Parkinson's disease. *FEBS J* 2012; 279: 1156–1166.
- Marin C, Aguilar E, Mengod G, Cortés R, Rodríguez-Oroz MC, Obeso JA. Entacapone potentiates the long-duration response but does not normalize levodopa-induced molecular changes. *Neurobiol Dis* 2008; 32: 340–348.
- Marin C, Aguilar E, Mengod G, Cortés R, Obeso JA. Effects of early vs late initiation of levodopa treatment in hemiparkinsonian rats. *Eur J Neurosci* 2009; 30: 823–832.
- Datla KP, Blunt SB, Dexter DT. Chronic L-DOPA administration is not toxic to the remaining dopaminergic nigrostriatal neurons, but instead may promote their functional recovery, in rats with partial 6-OHDA or FeCl(3) nigrostriatal lesions. *Mov Disord* 2001; 16: 424–434.
- Kemmerer ES, Desmond TJ, Albin RL, Kilbourn MR, Frey KA. Treatment effects on nigrostriatal projection integrity in partial 6-OHDA lesions: comparison of L-DOPA and pramipexole. *Exp Neurol* 2003; 183: 81–86.
- Murer MG, Dziewczapolski G, Menalled LB, Garcia MC, Agid Y, Gershanik O, Raisman-Vozari R. Chronic levodopa is not toxic for remaining dopamine neurons, but instead promotes their recovery, in rats with moderate nigrostriatal lesions. *Ann Neurol* 1998; 43: 561–575.
- Nguyen TV, Brownell AL, Iris Chen YC, Livni E, Coyle JT, Rosen BR, Cavagna F, Jenkins BG. Detection of the effects of dopamine receptor supersensitivity using pharmacological MRI and correlations with PET. *Synapse* 2000; 36: 57–65.
- Hume SP, Lammertsma AA, Myers R, Rajeswaran S, Bloomfield PM, Ashworth S, Fricker RA, Torres EM, Watson I, Jones T. The potential of high-resolution positron emission tomography to monitor striatal dopaminergic function in rat models of disease. *J Neurosci Meth* 1996; 67: 103–112.
- Cicchetti F, Brownell AL, Williams K, Chen YI, Livni E, Isacson O. Neuroinflammation of the nigrostriatal pathway during progressive 6-OHDA dopamine degeneration in rats monitored by immunohistochemistry and PET imaging. *Eur J Neurosci* 2002; 15: 991–998.
- Inaji M, Okauchi T, Ando K, Maeda J, Nagai Y, Yoshizaki T, Okano H, Nariai T, Ohno K, Obayashi S, Higuchi M, Suhara T. Correlation between quantitative imaging and behavior in unilaterally 6-OHDA-lesioned rats. *Brain Res* 2005; 1064: 136–145.
- Pellegrino D, Cicchetti F, Wang X, Zhu A, Yu M, Saint-Pierre M, Brownell AL. Modulation of dopaminergic and glutamatergic brain function: PET studies on parkinsonian rats. *J Nucl Med* 2007; 48: 1147–1153.
- Forsback S, Niemi R, Marjamäki P, Eskola O, Bergman J, Grönroos T, Haaparanta M, Haapalinna A, Rinne J, Solin O. Uptake of 6-[18F] fluoro-Ldopa and [18F]CFT reflect nigral neuronal loss in a rat model of Parkinson's disease. *Synapse* 2004; 51: 119–127.
- Chen YK, Liu RS, Huang WS, Wey SP, Ting G, Liu JC, Shen YY, Wan FJ. The role of dopamine transporter imaging agent [99mTc]TRODAT-1 in hemi-parkinsonism rat brain. *Nucl Med Biol* 2001; 28: 923–928.
- Choi JY, Kim CH, Jeon TJ, Cho WG, Lee JS, Lee SJ, Choi TH, Kim BS, Yi CH, Seo Y, Yi DI, Han SJ, Lee M, Kim DG, Lee JD, An G, Ryu YH. Evaluation of dopamine transporters and D2 receptors in hemiparkinsonian rat brains *in vivo* using consecutive PET scans of [18F]FPCIT and [18F]fallypride. *Appl Radiat Isot* 2012; 70: 2689–2694.
- Booij J, de Bruin K, Habraken JB, Voorn P. Imaging of dopamine transporters in rats using high-resolution pinhole single-photon emission tomography. *Eur J Nucl Med Mol Imag* 2002; 29: 1221–1224.

27. Scherfler C, Donnemiller E, Schocke M, Dierkes K, Decristoforo C, Oberladstätter M, Kolbitsch C, Zschiegner F, Riccabona G, Poewe W, Wenning G. Evaluation of striatal dopamine transporter function in rats by *in vivo* β -[¹²³I]CIT pinhole SPECT. *Neuroimage* 2002; 7: 128–141.
28. Van Camp N, Vreys R, Van Laere K, Lauwers E, Beque D, Verhoye M, Casteels C, Verbruggen A, Debyser Z, Mortelmans L, Sijbers J, Nuyts J, Baekelandt V, Van der Linden A. Morphologic and functional changes in the unilateral 6-hydroxydopamine lesion rat model for Parkinson's disease discerned with microSPECT and quantitative MRI. *MAGMA* 2010; 23: 65–75.
29. Bäck S, Raki M, Tuominen RK, Raasmaja A, Bergström K, Männistö PT. High correlation between *in vivo* [¹²³I] β -CIT SPECT/CT imaging and post-mortem immunohistochemical findings in the evaluation of lesions induced by 6-OHDA in rats. *EJNMMI Res* 2013; 3: 46.
30. Gleave JA, Farncombe TH, Saab C, Doering LC. Correlative single photon emission computed tomography imaging of [¹²³I]altropine binding in the rat model of Parkinson's. *Nucl Med Biol* 2011; 38: 741–749.
31. Nikolaus S, Larisch R, Vosberg H, Beu M, Wirrwar A, Antke C, Kley K, Silva MA, Huston JP, Müller HW. Pharmacological challenge and synaptic response – assessing dopaminergic function in the rat striatum with small animal single-photon emission computed tomography (SPECT) and positron emission tomography (PET). *Rev Neurosci* 2011; 22: 625–645.
32. Park E. A new era of clinical dopamine transporter imaging using [¹²³I]FP-CIT. *J Nucl Med Technol* 2012; 40: 222–228.
33. Tseng KY, Kargieman L, Gacio S, Riquelme LA, Murer MG. Consequences of partial and severe dopaminergic lesion on basal ganglia oscillatory activity and akinesia. *Eur J Neurosci* 2005; 22: 2579–2586.
34. Depboylu C, Maurer L, Matusch A, Hermanns G, Windolph A, Béhé M, Oertel WH, Höglinger GU. Effect of long-term treatment with pramipexole or levodopa on presynaptic markers assessed by longitudinal [¹²³I]FP-CIT SPECT and histochemistry. *Neuroimage* 2013; 79: 191–200.
35. Soria G, Aguilar E, Tudela R, Mullol J, Planas AM, Marin C. *In vivo* magnetic resonance imaging characterization of bilateral structural changes in experimental Parkinson's disease: a T2 relaxometry study combined with longitudinal diffusion tensor imaging and manganese-enhanced magnetic resonance imaging in the 6-hydroxydopamine rat model. *Eur J Neurosci* 2011; 33: 1551–1560.
36. Kondoh T, Bannai M, Nishino H, Torii K. 6-Hydroxydopamine-induced lesions in a rat model of hemi-Parkinson's disease monitored by magnetic resonance imaging. *Exp Neurol* 2005; 192: 194–202.
37. Paxinos G, Watson C. *The Rat Brain in Stereotaxic Coordinates*. Academic Press: New York, 1998.
38. Papa SM, Engber TM, Kask AM, Chase TN. Motor fluctuations in levodopa-treated parkinsonian rats: relation to lesion extent and treatment duration. *Brain Res* 1994; 662: 69–74.
39. Pino F, Roé N, Orero A, Falcón C, Rojas S, Benlloch JM, Ros D, Pavia J. Development of a variable-radius pinhole SPECT system with a portable gammacamera. *Rev Esp Med Nucl* 2011; 30: 286–291.
40. Booij J, Andringa G, Rijks LJ, Vermeulen RJ, De Bruin K, Boer GJ, Janssen AG, Van Royen EA. [¹²³I] FP-CIT binds to the dopamine transporter as assessed biodistribution studies in rats and SPECT studies in MPTP-lesioned monkeys. *Synapse* 1997; 27: 183–190.
41. Lage E, Villena JL, Tapias G, Martínez NP, Soto-Montenegro ML, Abella M, Sisniega A, Pino F, Ros D, Pavia Javier, Desco M, Vaquero JJ. A SPECT scanner for rodent imaging based on small-area gamma cameras. *IEEE Tans Nucl Sci* 2010; 57: 2524–2531.
42. Rubins DJ, Melega WP, Lacan G, Way B, Plenevaux A, Luxen A, Cherry SR. Development and evaluation of an automated atlas-based image analysis method for microPET studies of the rat brain. *Neuroimage* 2003; 20: 2100–2118.
43. Rojas S, Martín A, Pareto D, Herance JR, Abad S, Ruíz A, Flotats N, Gispert JD, Llop J, Gómez-Vallejo V, Planas AM. Positron emission tomography with [¹¹C]flumazenil in the rat shows preservation of binding sites during the acute phase after 2 h-transient focal ischemia. *Neuroscience* 2011; 182: 208–216.
44. Martín A, Gómez-Vallejo V, San Sebastián E, Padró D, Markuerkiaga I, Larena I, Llop J. *In vivo* imaging of dopaminergic neurotransmission after transient focal ischemia in rats. *J Cereb Blood Flow Metab* 2013; 33: 244–252.